LCST behaviour in blends of poly(vinylidene fluoride) and isotactic poly(ethyl methacrylate)

E. Roerdink and G. Challa
Laboratory of Polymer Chemistry, Mjenborgh 16, Groningen, The Netherlands
(Received 4 December 1979)

Blends of poly(vinylidene fluoride) (PVF_2) with isotactic, atactic or syndiotactic poly(ethyl methacrylate) (it-, at- or st-PEMA) were studied by calorimetry and light microscopy. The occurrence of single glass transitions over a broad composition, as well as the lowering of the crystallization temperature upon cooling from the melt, indicate a complete compatibility in the amorphous state in blends of PVF_2 with at- and st-PEMA up to high temperatures. With it-PEMA, however, phase separation took place when the temperature was raised, sugesting LCST behaviour. Cloud points appeared in the temperature range of 150–200°C, making this system suitable for phase separation studies. The occurrence of double glass transitions as well as double crystallization exotherms in some PVF_2/it-PEMA blends could be explained from the phase diagram and the slowness of phase mixing upon cooling.

INTRODUCTION

Among the polymer blends which exhibit lower critical solution temperature (LCST) behaviour, polystyrene/poly(vinyl methyl ether)[1], polycaprolactone/poly(styrene-co-acrylonitrile)[2] and poly(methyl methacrylate)/-poly(styrene-co-acrylonitrile)[3] are the most well known examples. LCST behaviour has also been reported in blends of poly(vinylidene fluoride) (PVF_2) with several poly(alkyl methacrylates), especially atactic poly(ethyl methacrylate)[4,5]. Compatibility between PVF_2 and at-PEMA in the molten state has already been reported by several authors[6–8]. The results of these studies indicate that homogeneous blends of PVF_2 with at-PEMA become heterogeneous by crystallization of PVF_2 upon cooling from the melt. In one paper the occurrence of an upper critical solution temperature (UCST) was suggested[7], but no experimental evidence has so far been found to support this hypothesis. The influence of tacticity on the compatibility of two polymers has already been studied for poly(methyl methacrylate)/poly(vinyl chloride) (PMMA/PVC) and PMMA/PVF_2 systems[9,10]. In the former case, differences in compatibility between the it- and st-PMMA with PVC have been established, while in the second system a difference in binary interaction parameter of the stereoregular PMMAs with respect to PVF_2 has been measured. As the position of UCST and LCST is strongly dependent on the binary interaction parameter[2], differences in compatibility of stereoregular PEMAs with PVF_2 could also be expected and therefore a study was performed on the compatibility of PVF_2 with stereoregular PEMAs.

EXPERIMENTAL

Isotactic (it-) PEMA polymers were prepared with phenylmagnesiumbromide as Grignard initiator in toluene at 25°C, according to Goode *et al.*[11]. Syndiotactic (st-) PEMA was prepared by a Ziegler–Natta polymerization at −78°C in toluene with triethylaluminium and titaniumtetrachloride as catalysts. The procedure of Abe *et al.*[12] was followed in the preparation of st-PEMA. Atactic (at-)PEMA was obtained by an ordinary radical polymerization of ethylmethacrylate monomer in a 12.5 volume% toluene solution at 50°C with 0.01 mol dm^{-3} bis(*p*-tert-butylcyclohexyl) dipercarbonate as initiator. PVF_2 was the KF resin from Kureha Chemical Industry Co. Ltd. and was the same as that used previously[10].

The tacticities of the PEMA samples were derived from the 100 MHz n.m.r. spectra, recorded on 1 wt% polymer solutions at 58°C in $CDCl_3$ with a Varian XL-100 spectrometer by using a peak elimination technique. This technique was first described by Hatada *et al.*[13] for poly(alkyl methacrylates) and also applied by Bosscher *et al.* to poly(ethyl-) and poly(isobutyl methacrylates)[14]. $[\eta]$ of the PEMA polymers were determined in methyl ethyl ketone at 23°C. For the calculation of $\bar{M}_v$ the relationship $[\eta] = 2.83 \times 10^{-5} (\bar{M}_v)^{0.79}$ was used[15]. The data of the used PEMAs are collected in *Table* 1. Blends of PVF_2 with it-, at- and st-PEMA were prepared as described previously for PVF_2/PMMA blends[10]. All compositions of the blends are indicated as weight percentages, e.g. a 40–60 PVF_2/it-PEMA blend. Also the determination of melting, crystallization and glass-transition temperatures by d.s.c. were performed as described in this reference.

0032-3861/80/101161-06$02.00

Table 1 Data of PEMA polymers used

	$[\eta]$ (dl/g)	$\bar{M}_v \times 10^{-3}$	triads *I*	*H*	*S*
it–PEMA–1	0.28	115	93	5	2
it–PEMA–2	0.39	172	99	1	0
at–PEMA	0.12	38	5	38	57
st–PEMA	0.24	93	2	13	85

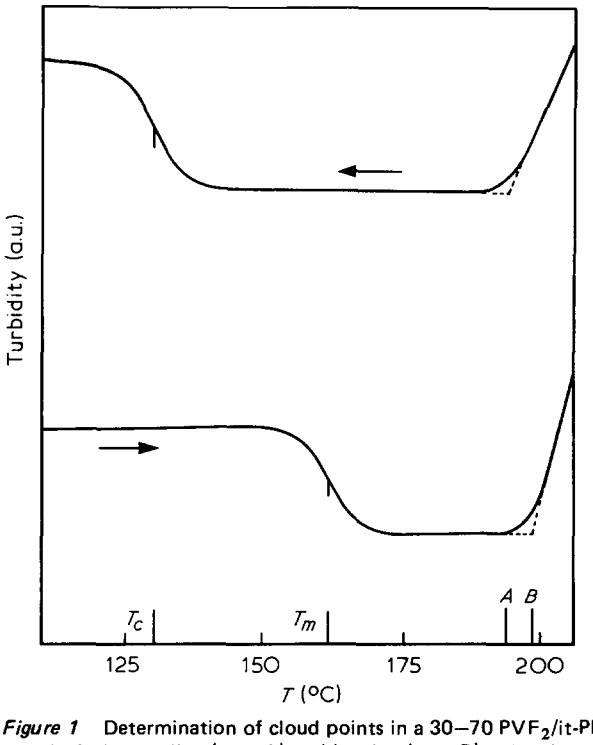

Figure 1 Determination of cloud points in a 30–70 PVF_2/it-PEMA sample during cooling (⇐, A) and heating (⇒, B) at heating and cooling rates of 3° min^{-1}

Cloud points in blends of PVF_2 with high it-PEMA content (>40 wt%) were recorded by following the turbidity of thin polymer films of given composition as a function of temperature in a hot stage plate (Mettler FP5). For this purpose, a light dependent resistance (LDR) connected in a Wheatstone bridge was placed in the tube of a Zeiss microscope. Cloud points appeared as a sudden increase in turbidity upon heating and a decrease in turbidity upon cooling the samples (see *Figure* 1). Melting and crystallization temperatures could also be derived from the turbidigrams and they proved to be in good agreement with the d.s.c. results.

Cloud points in blends of PVF_2 with low it-PEMA content (<20 wt%) could not be detected in the above way, because no sharp transition point was observed. For these blends, the cloud point at a given temperature was detected by plotting turbidity versus composition as demonstrated in *Figure* 2. To that end, films of blends with low it-PEMA contents and ~100 μm thick were placed in a Leitz hot stage microscope and kept at constant temperature until the transmittance was constant. The turbidity was expressed as $1/t \ln I_0/I$, where I_0/I is the intensity ratio of the incoming and passing light and t is the thickness of the film.

RESULTS

Turbidity measurements

In *Figure* 1 the turbidity of a 30–70 PVF_2/it-PEMA sample is represented in a temperature cycle with heating and cooling rates of 3° min^{-1}. In general, the cloud points (B) registered during heating were ~5°C higher than the cloud points (A) registered during cooling. As crystallization temperatures (T_c) observed during cooling were lower than melting temperatures (T_m) during subsequent heating, cloud points could be detected up to higher PVF_2 contents upon cooling than upon heating. However, at PVF_2 contents higher than 60 wt%, the crystallization process interfered with the phase mixing upon cooling, and the turbidigram was no longer interpretable. From turbidigrams such as *Figure* 1, cloud points could be detected in blends with a wt% it-PEMA > 40. In *Figure* 2, the turbidity of blends at 200°C is plotted as a function of wt% it-PEMA. From such figures, cloud points could be derived in the low it-PEMA content range of the phase diagram. In *Figure* 3 the whole phase diagram as recorded by turbidity measurements is presented.

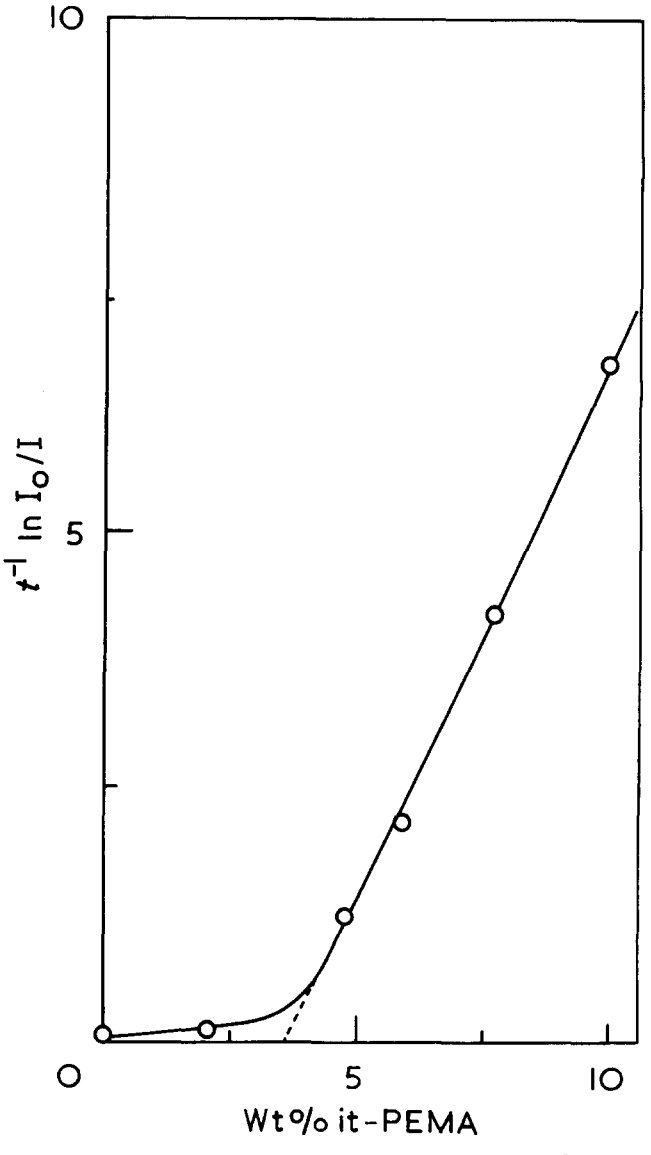

Figure 2 Isothermal determination of a cloud point at 200°C in blends of PVF_2 with it-PEMA

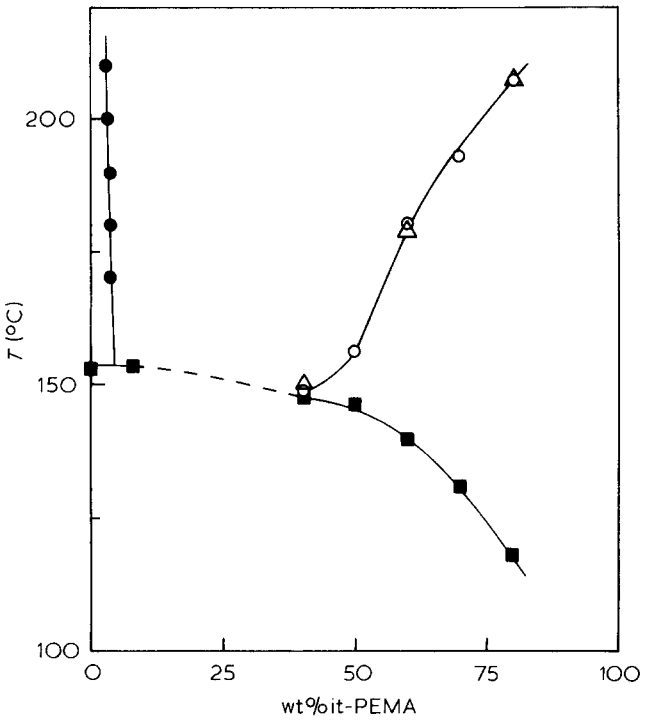

Figure 3 Cloud point curve of blends of PVF_2 with it-PEMA-2 (○, ●) and it-PEMA-1 (△), recorded by turbidimetry either isothermal (●) or at a cooling rate of 3° min^{-1} (○, △). ■, Crystallization temperatures (T_c) of blends of PVF_2 with it-PEMA-2, recorded by turbidimetry at a cooling rate of 3° min^{-1}

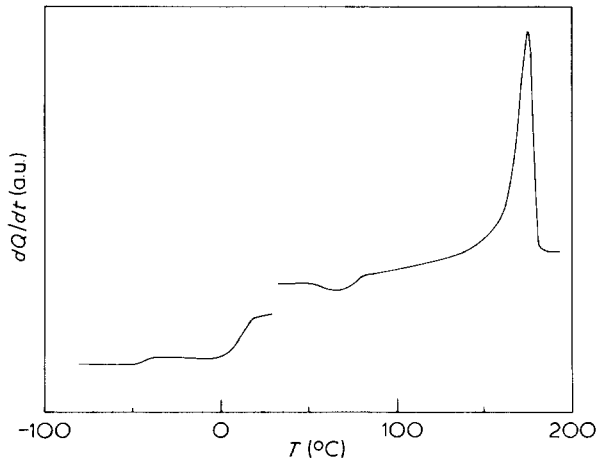

Figure 4 Thermogram of an 80–20 PVF_2/it-PEMA blend recorded by d.s.c. at a heating rate of 10° min^{-1} for the glass transitions and 20° min^{-1} for crystallization and melting. Glass transitions are recorded at a 10 times higher sensitivity of the d.s.c. apparatus

In PVF_2/at-PEMA and PVF_2/st-PEMA blends, no cloud points could be observed up to temperatures of 250°C.

T_g measurements of quenched samples

Blends of PVF_2 with it- or st-PEMA were quenched from the molten state at 200°C in liquid nitrogen to suppress crystallization of PVF_2 from the blends. After quenching, the glass transition was recorded during heating and the d.s.c. scan was continued. The crystallization exotherm area, which was present in some of the blends, was subtracted from the area of the subsequent melting endotherm to derive the relative crystallinity of PVF_2 during the glass transition (*Figure* 4). None of the PVF_2/it-PEMA blends appeared to be completely amorphous, while in blends of PVF_2 with st-PEMA only the samples with wt% $PVF_2 > 80$ were partly crystalline. In blends of PVF_2 with rather low it-PEMA contents, clearly two T_g's were observed (*Figures* 4 and 5). The c_p jump of the lower glass transition was comparable in size and shape with that of pure PVF_2 in a partly crystalline state. The upper T_g is lowered by 6°C at most, with respect to the T_g of pure it-PEMA.

In blends of PVF_2 and st-PEMA one T_g was observed in all blends, decreasing smoothly with composition with respect to the T_g of pure st-PEMA (*Figure* 6). Comparable results were obtained in blends of PVF_2 with at-PEMA.

Crystallization of PVF_2 from the blends

Upon cooling molten blends of PVF_2 with at- and st-PEMA one single crystallization exotherm was observed, which shifted to lower temperature with increasing PEMA content (*Figure* 7). In blends of PVF_2 with it-PEMA, the crystallization behaviour is more complicated. In the 80–20 PVF_2/it-PEMA blend one crystallization exotherm was observed at the same temperature as the pure PVF_2 crystallization exotherm. At higher it-PEMA contents an additional exotherm arose at lower temperatures. Finally, in the 20–80 PVF_2/it-PEMA blend again only one crystallization exotherm is found, at relatively low temperature. The double crystallization phenomenon appeared to be dependent on the cooling rate. This feature is shown in *Figure* 8, where d.s.c. scans of a 40–60 PVF_2/it-PEMA sample during cooling from the melt are represented for various cooling rates. As the cooling rate decreases, crystallization of PVF_2 takes place at smaller supercooling and besides, both crystallization exotherms gradually coincide. At a cooling rate of 0.31° min^{-1}, one single crystallization exotherm was observed in this blend at 155°C which is still far below the cloud point at 180°C (*Figure* 3). When the PVF_2/it-PEMA samples were kept for a longer time at a temperature well above the cloud point, two phases became visible under the microscope,

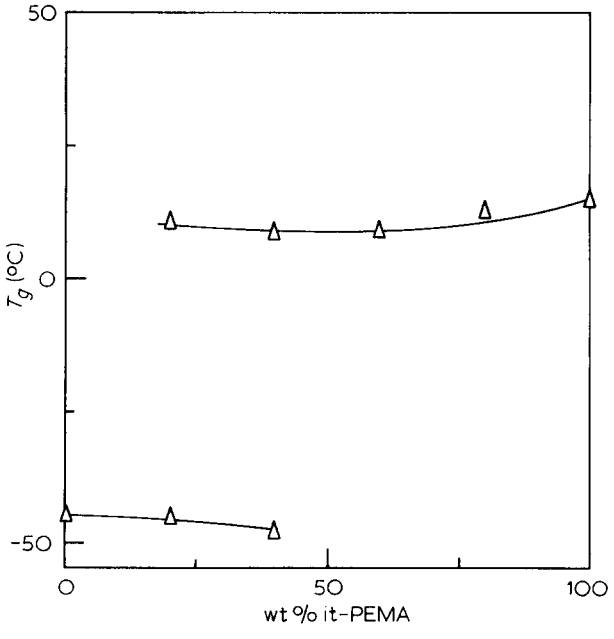

Figure 5 Glass transition temperatures (T_g) of PVF_2/it-PEMA blends after quenching from the melt in liquid nitrogen.

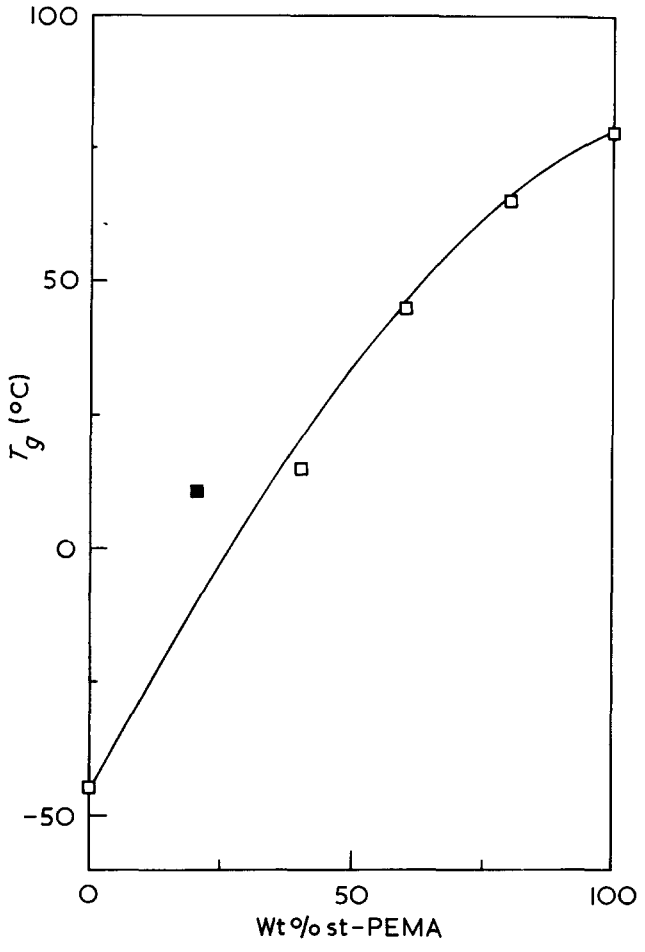

Figure 6 Glass transition temperatures (T_g) of PVF_2/st-PEMA blends after quenching from the melt in liquid nitrogen. The solid line is calculated with the theoretical Gordon–Taylor relation. A filled symbol (■) is used for the partly crystalline 80–20 PVF_2/st-PEMA blend

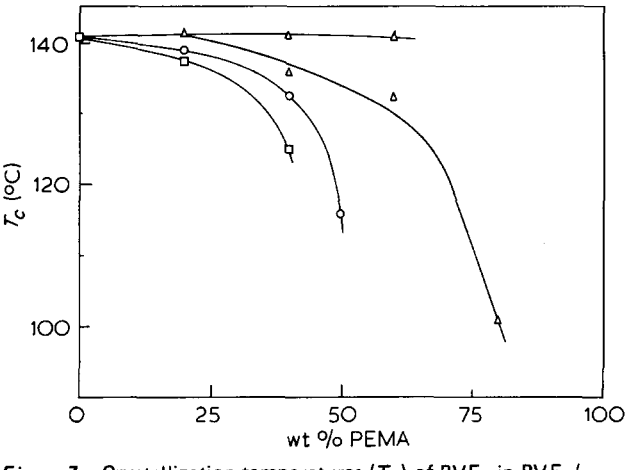

Figure 7 Crystallization temperatures (T_c) of PVF_2 in PVF_2/PEMA blends measured during cooling in d.s.c. at 8° min^{-1}; △, PVF_2/it-PEMA-1; ○, PVF_2/at-PEMA; □, PVF_2/st-PEMA

one of which appeared to be rich in PVF_2 and the other one poor in PVF_2. This is best illustrated by quickly quenching such a sample to room temperature. The PVF_2-rich phase crystallizes in an infinite number of small spherulites whereas the PVF_2-poor phase remains amorphous. Between crossed polarizers such a quenched sample displayed amorphous islands of ~100 μm in diameter dispersed in a birefringent matrix as shown in *Figure* 9 for a 60–40 PVF_2/it-PEMA sample. Photographs like *Figure* 9 enable us to control the reliability of the cloud point curve. From *Figure* 3 it follows that in the case of phase separation in a 60–40 PVF_2/it-PEMA sample at 210°C, the two coexisting phases should contain 3.0 and 83.0 wt% it-PEMA and should be present in a weight ratio of 0.54/0.46. With densities of 1.95 and 1.68 g cm^{-3} for partly crystalline and pure amorphous PVF_2 respectively[16,17], and 1.11 g cm^{-3} for it-PEMA (literature value for at-PEMA[18]), the calculated densities for the PVF_2-rich and the PVF_2-poor phase at room temperature amount to 1.907 and 1.178, respectively. The volume fraction of the PVF_2-poor phase is then calculated as follows:

$$\phi PVF_2\text{-poor phase} = (0.46/1.178) \times$$

$$(0.46/1.178 + 0.54/1.907)^{-1} = 0.58$$

This value is in perfect agreement with 0.58 ± 0.03 as determined from 3 photographs, like those in *Figure* 9, of a quenched 60–40 PVF_2/it-PEMA sample, kept for 12 h at 210°C. When PVF_2 is crystallized after complete phase separation, this results in differences in size and birefringence of the spherulites in both phases. For example, a 40–60 PVF_2/it-PEMA sample was crystallized isothermally at 150°C after phase sparation at 190°C for 15 h. This thermal treatment yields a PVF_2-rich phase, wherein crystallization of PVF_2 has been completed, dispersed in a PVF_2-poor matrix with thin spherulites, still growing at a

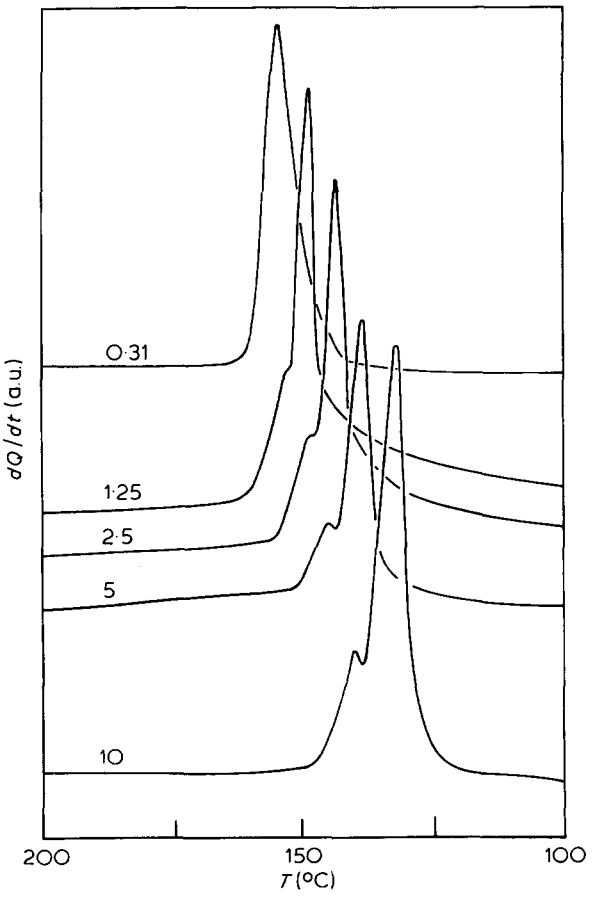

Figure 8 Crystallization exotherms of a 40–60 PVF_2/it-PEMA blend recorded by d.s.c. at different cooling rates as indicated in degrees per minute

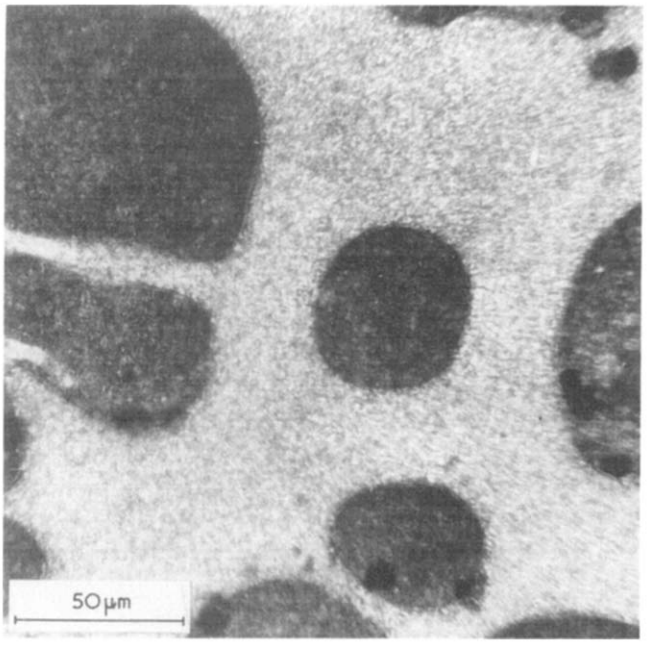

Figure 9 A 60–40 PVF_2/it-PEMA sample quenched to room temperature after phase separation for 15 h at 210°C, as observed between crossed Nicols in a light microscope. The nearly completely amorphous PVF_2-poor phase appears as dark spots in the birefringent, crystalline PVF_2-rich matrix

radial growth rate which is ~30 times lower than in the PVF_2-rich phase (*Figure* 10). Compared with the 60–40 blend shown in *Figure* 9, inversion of the matrix and dispersed phases has taken place. By adjusting the phase separation time and temperature it turned out to be possible to create different sizes for the two different phases, as well as to vary the mutual composition. It also appeared to be possible to vary the spherulitic size by choosing proper crystallization temperatures for the two phases, as shown by the two extreme situations in *Figures* 9 and 10 with $T_c = 20$ and 150°C respectively.

DISCUSSION

PVF_2/it-PEMA blends exhibit an LCST (*Figure* 3). Although this cloud point curve supplies an indication for the position of the critical point the exact position cannot be localized for these particular polymers because of the interfering crystallization of PVF_2. However, with it-PEMA of much lower molecular mass, the cloud point curve (CPC) might be lifted above the crystallization line.

The tacticity of the PEMA polymers should have a much stronger influence on the CPC than the molecular mass. This originates from the strong dependence of the binary interaction parameter on tacticity, as theoretically predicted by McMaster[2]. The complete compatibility of st-PEMA with PVF_2 (see *Figure* 6) suggests more favourable interaction of PVF_2 with st-PEMA than with it-PEMA. Therefore, the LCST for the PVF_2/st-PEMA system is probably localized at a much higher temperature than the LCST for the PVF_2/it-PEMA system, while in blends with at-PEMA an intermediate position for the LCST can be expected[6]. However, as our at-PEMA was subjected to strong thermal degradation at temperatures above ~200°C, it was impossible to determine the cloud points in blends of PVF_2 with at-PEMA.

In our measurements there was no strong dependence of the cloud points, in blends of PVF_2 with it-PEMA, on the cooling or heating rate. However, complete phase mixing after cooling was reached only at very low cooling rates, as concluded from the d.s.c. thermograms in *Figure* 8. At a high cooling rate, phase mixing is not reached completely and PVF_2 starts to crystallize firstly from the PVF_2-rich phase and, at larger supercooling, from the diluted phase. The smaller exotherm area, due to the crystallization of PVF_2 from the PVF_2-rich phase, is in line with the phase diagram in *Figure* 3 which predicts a minor amount of PVF_2-rich phase at temperatures just above the cloud point. As the cooling rate is decreased, the two phases become better mixed so that the two different crystallization exotherms coincide. The occurrence of double crystallization exotherms in other PVF_2/it-PEMA blends as illustrated in *Figure* 7 can be explained from this. As these blends were cooled from 200°C at a relatively high cooling rate (8°C min^{-1}), two phases can be expected in blends with an it-PEMA content between 3.5 and 75.0 wt% (see *Figure* 3). So, the upper crystallization exotherm can be ascribed to the PVF_2-rich phase, and the lower one to the PVF_2-poor phase. The same explanation holds for the T_g analysis of the PVF_2/it-PEMA blends, quenched from the molten state at 200°C into liquid nitrogen (*Figure* 5). However, because of the low melt viscosity of these blends, which in turn is related to the low T_g's of both polymers[18], crystallization of PVF_2 could not be avoided, even in blends with low PVF_2 content. This phenomenon affects the T_g analysis in the following way: at high it-PEMA content blends are homogeneous in the molten state at 200°C and upon quenching a part of the PVF_2 crystallizes leading to a somewhat higher it-PEMA content in the remaining amorphous phase than suggested by the overall composition. Therefore, one single glass-transition is observed in such blends which is slightly lowered with respect to pure it-PEMA. Blends with lower it-PEMA content are heterogeneous at 200°C as a result of liquid–liquid phase separation. Upon quenching in liquid nitrogen part of the PVF_2 crystallizes in both phases leading to two T_g's which belong to the remaining amorphous part of these phases. Blends of PVF_2 and at- and st-PEMA are homogeneous above the melting point of PVF_2 as indicated by the absence of any turbidity in these blends, as well as by the lowering of the crystallization temperature with respect to undiluted PVF_2

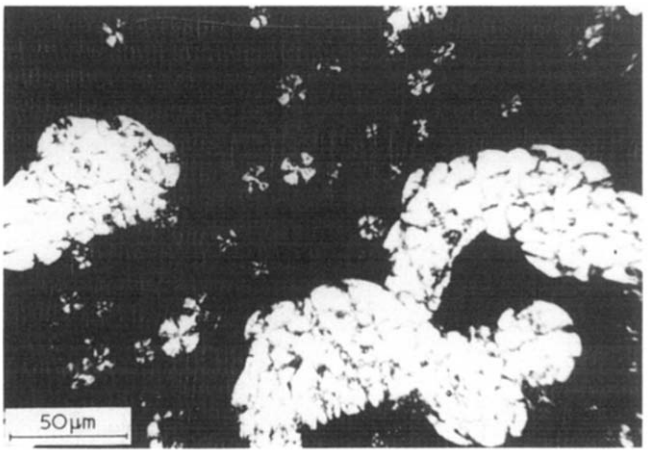

Figure 10 A 40–60 PVF_2/it-PEMA sample, isothermally crystallized at 150°C after phase separation at 190°C

(*Figure* 7). Although degradation of at-PEMA at 200°C may complicate the interpretation, the idea of compatibility in amorphous blends of PVF_2 with at- and st-PEMA is also supported by the occurrence of one single glass transition over a large composition range (*Figure* 6). Extrapolation to the T_g of pure PVF_2 at −45°C might be hampered by the relative high T_g value of the 80–20 PVF_2/st-PEMA blend. However, as a part of the PVF_2 is crystallized from this PVF_2-rich blend, the remaining amorphous phase becomes richer in PEMA, leading to a higher T_g than would be expected according to the overall composition, Similar phenomena were perceived in blends of PVF_2 with it-, at- and st-PMMAs. At high PVF_2 contents T_g's differing from the theoretical Gordon–Taylor relation[20], were observed in addition to broad transitions attributed to the molecular motions of cilia, loose loops etc. on crystal surfaces of PVF_2.

Extrapolation of the T_g values in homogeneous blends of PVF_2 with at-PEMA or with some poly(alkyl acrylates) to the T_g value of pure PVF_2 at −45°C is not accepted in some cases[8,19]. To emphasize that his extrapolation is justified we applied the theoretical Gordon–Taylor relation[20]

$$T_g=(c_2T_{g_2}+c_1kT_{g_1})/(c_2+c_1k)$$

to the T_g values of PVF_2/st-PEMA blends. In this relation, subscript 1 indicates the polymer with the higher T_g (st-PEMA) and subscript 2 the polymer with the lower T_g (PVF_2), c=weight fraction, $k=\Delta_1 e/\Delta_2 e=(e_l-e_g)_1/(e_l-e_g)_2$, $e_{l,g}=(\delta v/\delta T)_p$, the thermal specific expansivity in the liquid and the glassy state, respectively (dim. cm^3/gK). Within about 5°C, all T_g values of the amorphous PVF_2/st-PEMA blends could be adapted to the Gordon–Taylor relation, by taking $k=1.8$. With our value $\Delta e_2=1.9\pm0.1\times10^{-4}$ for amorphous PVF_2 (see ref. 10), the calculated Δe_1 value for st-PEMA amounts then 3.4×10^{-4}, which is only slightly higher than the literature value $2.6-2.9\times10^{-4}$ for at-PEMA[21]. So, at least for PVF_2/st-PEMA blends, extrapolation of the T_g values to the T_g of PVF_2 at −45°C seems to be justified in a way which is comparable to the extrapolation of the T_g values of blends of PVF_2 and at-PEMA in the study of Noland *et al.*[6], based upon the Kelley-Bueche equation[22].

Although the results of the glass transition analysis of the PVF_2/it- and st-PEMA blends can be explained by phase separation at high temperature in the PVF_2/it-PEMA system coupled to a crystallization of PVF_2 from all blends in the PVF_2/it-PEMA system and from some PVF_2-rich blends of the PVF_2/st-PEMA system, the occurrence of an UCST as suggested by Kwei *et al.*[7] for the PVF_2/at-PEMA cannot be excluded completely. This should imply inversion of the sign of the binary interaction parameter from negative (LCST) to positive (UCST) upon lowering the temperature. The complete compatibility of st-PEMA with PVF_2 indicates a more negative binary interaction parameter for PVF_2 with st-PEMA that with it-PEMA and as a consequence the occurrence of an UCST would be expected in blends of PVF_2 with it-PEMA rather than with st-PEMA. So, by applying it-PEMAs with different molecular weights, the exact position of LCST and perhaps the occurrence of an USCT might be studied in more detail.

REFERENCES

1 Bank, M., Leffingwell, J. and Thies, C. *J. Polym. Sci.* (*A*-2) 1972, **10**, 1097
2 McMaster, L. P. *Macromolecules* 1973, **6**, 760
3 McMaster, L. P. *Adv. Chem. Ser.* 1975, **142**, 43
4 Bernstein, R. E., Cruz, C. A., Paul, D. R. and Barlow, J. W. *Macromolecules* 1977, **10**, 681
5 Paul, D. R., Barlow, J. W., Bernstein, R. E. and Wahrmund, D. C. *Polym. Eng. Sci.* 1978, **18**, 1225
6 Noland, J. S., Hsu, N. N. C., Saxon, R. and Schmitt, J. M. *Adv. Chem. Ser.* 1971, **99**, 15
7 Kwei, T. K., Patterson, G. W. and Wang, T. T. *Macromolecules* 1976, **9**, 780
8 Imken, R. L., Paul, D. R. and Barlow, J. W. *Polym. Eng. Sci.* 1976, **16**, 593
9 Schurer, J. W., de Boer, A. and Challa, G. *Polymer* 1975, **16**, 201
10 Roerdink, E. and Challa, G. *Polymer* 1978, **19**, 173
11 Goode, W. E., Owens, F. H., Feldmann, R. P., Snijder, W. H. and Moore, J. H. *J. Polym. Sci.* 1960, **46**, 317
12 Abe, H., Imai, K. and Matsumoto, M. *J. Polym. Sci.* (*C*) 1968, **23**, 469
13 Hatada, K., Ohta, K., Okamoto, Y., Kitayama, T., Umemura, Y. and Yhi, H. *J. Polym. Sci.* (*Polym. Lett. Edn*) 1976, **14**, 531
14 Bosscher, F., Keekstra, D. and Challa, G. to be published
15 Chinai, S. N. and Samuels, R. J. *J. Polym. Sci.* 1956, **19**, 463
16 Brandrup, J. and Immergut, E. H. 'Polymer Handbook', Wiley–Interscience, New York, 1966
17 Welch, G. J. and Miller, R. L. *J. Polym. Sci.* (*Polym. Phys. Edn*) 1976, **14**, 1683
18 Williams, M. L., Landel, R. F. and Ferry, J. D. *J. Am. Chem. Soc.* 1955, **77**, 3701
19 Warhmund, D. C., Bernstein, R. E., Barlow, J. W. and Paul, D. R. *Polym. Eng. Sci.* 1978, **18**, 677
20 Gordon, M. and Taylor, J. S. *J. Appl. Chem.* 1952, **2**, 493
21 Van Krevelen, D. W. 'Properties of Polymers', Elsevier, Amsterdam, 1976
22 Kelley, F. N. and Bueche, F. *J. Polym. Sci.* 1961, **50**, 549